

Cardiac MRI on the MAGNETOM Free.Max: The Ohio State Experience

Orlando P. Simonetti¹, Juliet Varghese¹, Ning Jin², Daniel Giese³, Yingmin Liu¹, Chong Chen¹, Rizwan Ahmad¹, Yuchi Han¹

¹The Ohio State University, Columbus, OH, USA

²Siemens Healthineers, Malvern, PA, USA

³Siemens Healthineers, Erlangen, Germany

Background

As the cardiovascular magnetic resonance (CMR) program at The Ohio State University has expanded, we added both a higher (3T, MAGNETOM Vida) and a lower (0.55T, MAGNETOM Free.Max) field system to our existing 1.5T MAGNETOM Sola. Having access to scanners with three different field strengths has enabled us to investigate the pros and cons of each across different CMR applications, with the aim to match the right field strength for the right patient and pathology. The first step in this process was to develop and implement cardiac imaging techniques for the MAGNETOM Free.Max, which was delivered without CMR product pulse sequences. We have worked closely with our colleagues at Siemens Healthineers to put together a comprehensive package of CMR techniques¹, which currently are still in the preliminary stage of development.

While signal-to-noise ratio (SNR) is directly proportional to the main magnetic field (B_0), lower B_0 offers a number of potential advantages for CMR [1, 2]. The higher field homogeneity and lower specific absorption rate (SAR) at lower-field benefits techniques that are dependent on balanced steady-state free precession (bSSFP), potentially increasing safety and reducing artifacts in patients with implanted devices². Lower B_0 means lower Lorentz forces, reducing audible noise and potentially improving the patient experience. Reduced B_0 also offers greater flexibility in magnet design. The Free.Max platform has a unique, 80 cm diameter bore and an optional 705 lb / 320 kg patient table limit, which eliminates barriers to MRI for those with severe obesity. One of our primary motivations to pursue the development of CMR techniques on the MAGNETOM Free.Max is to increase the accessibility to CMR for obese patients, as well as those with severe

claustrophobia who may benefit from the larger bore and quieter scans.

The United States Centers for Disease Control and Prevention (CDC) reports that the prevalence of obesity (body mass index (BMI) > 30 kg/m²) now exceeds 40% and is projected to affect 50% of the U.S. population by 2025 [3]. The obesity epidemic is not unique to the USA, with a prevalence now exceeding 20% in most Western European countries. Obesity increases the risk of cardiovascular disease (CVD) [4] and these risks are even greater in those with severe obesity, i.e., BMI > 40 kg/m², which now accounts for more than 9% of the adult USA population. This significant population segment faces serious healthcare challenges, especially in terms of access to non-invasive cardiovascular imaging. Most cardiac imaging equipment is not designed to accommodate the weight and girth of severely obese patients; furthermore, radiation-based modalities such as CT and SPECT require excessive radiation for adequate image quality, while attenuation of ultrasound by adipose tissue limits the utility of echocardiography [5, 6]. If not for the bore diameter (60 cm – 70 cm) and table weight limits (typically < 450 lbs / 200 kg) of standard magnetic resonance imaging (MRI) systems, MRI could provide a safe, comprehensive assessment of CVD in even the most severely obese patients. The 80 cm bore and optional 705 lb / 320 kg table weight limit of MAGNETOM Free.Max offer this possibility.

Several years ago, our group recognized the potential for low-field cardiovascular MRI [1], and demonstrated the feasibility of CMR at 0.35T in comparison with standard field strengths [7]. Our work, together with preliminary results published by others using a prototype scanner

¹Work in progress: the application is currently under development and is not for sale in the U.S. and in other countries. Its future availability cannot be ensured.

²The MRI restrictions (if any) of the metal implant must be considered prior to patient undergoing MRI exam. MR imaging of patients with metallic implants brings specific risks. However, certain implants are approved by the governing regulatory bodies to be MR conditionally safe. For such implants, the previously mentioned warning may not be applicable. Please contact the implant manufacturer for the specific conditional information. The conditions for MR safety are the responsibility of the implant manufacturer, not of Siemens Healthineers.

ramped-down to 0.55T [2, 8], supported the concept that high quality CMR could be feasible at reduced field strength. We hypothesized that the ultra-wide bore MAGNETOM Free.Max system could deliver the proven benefits of CMR to the severely obese patient population, i.e., patients who face significantly limited diagnostic image quality and radiation dosing challenges from other imaging modalities, and set a goal of developing a comprehensive suite of CMR techniques for the MAGNETOM Free.Max. To achieve this goal, however, requires overcoming two primary technical challenges;

- 1) the deficit in SNR as compared to higher field systems, and
- 2) the reduced gradient performance (26 mT/m max. amplitude and 45 mT/m/ms max. slew rate) of MAGNETOM Free.Max, resulting in longer echo times (TE) and repetition times (TR).

Taken together, these performance differences can lead to significantly longer scan times, and compromised spatial and temporal resolution. These factors are especially critical in CMR where scan time is often limited to a short breath-hold to avoid respiratory motion, and sufficient temporal resolution is required to avoid cardiac motion artifact, or to accurately resolve cardiac motion and flow. The initial steps we have taken to address these limitations include the implementation of dedicated pulse sequences, optimization of scan parameters, judicious use of advanced reconstruction strategies, and machine learning driven denoising. Preliminary results are shown in the following sections where we review the various component techniques that comprise the comprehensive cardiac package, and present example results we have obtained to date in animal models, healthy volunteers, and patients with cardiovascular disease, including those with severe obesity.

Our cardiac package

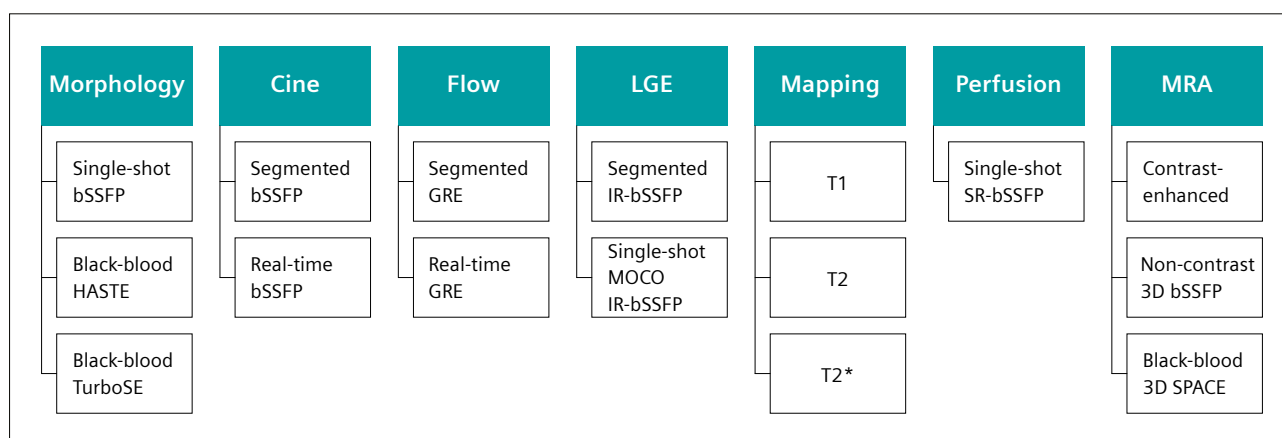
Overview

As the MAGNETOM Free.Max does not include dedicated sequences released for cardiac imaging, all of the following sequences and reconstruction techniques are research packages¹ that were enabled and/or developed by our group in collaboration with Siemens Healthineers. Furthermore, the MAGNETOM Free.Max does not have an integrated ECG triggering system; yet, it is capable of accepting an external triggering signal, and this can be provided by a variety of third-party patient monitoring systems.

At this early stage of the project, we have developed working techniques covering all of the clinical CMR applications shown in Figure 1. Our ultimate goal is to run protocols that obviate the need for patient breath-hold, and can be completed within 30 minutes; however, at this stage of development, some methods still rely on conventional segmented *k*-space, breath-hold acquisition. As we continue to innovate and combine advanced compressed sensing (CS) and deep learning-based reconstruction techniques paired with custom data acquisition strategies, we fully expect to achieve our goal of a rapid, comprehensive free-breathing CMR suite.

Morphology

Dark-blood turbo spin echo (TSE) based techniques are useful to distinguish morphological features and to characterize masses and tumors. The limited SNR and gradient speed available on MAGNETOM Free.Max impact the performance of some CMR techniques more than others. Given that TSE images tend to have relatively high SNR and the sequence is not reliant on fast gradients, the translation from higher field and faster gradient systems was

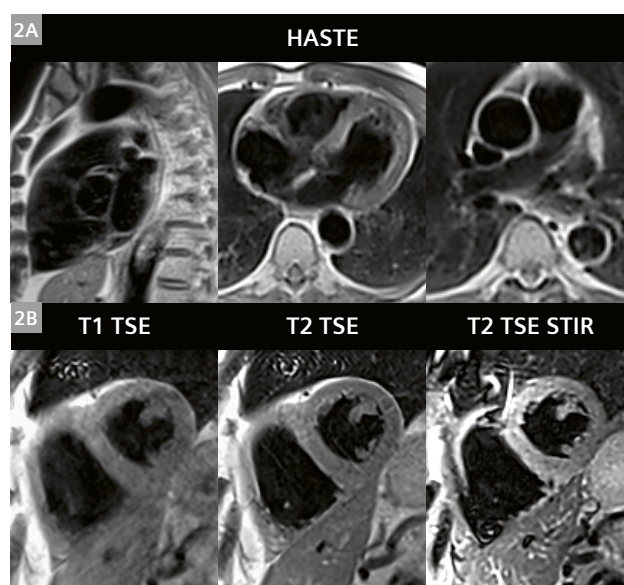


¹ Shown are the primary components of the comprehensive cardiac imaging package¹. All of the basic components are in place, although many of these techniques rely on breath-hold, segmented *k*-space acquisitions. Optimization of techniques and scan parameters is ongoing in our effort to maximize SNR, contrast, and image quality. We also continue working to develop strategies to support free-breathing image acquisition across all categories.

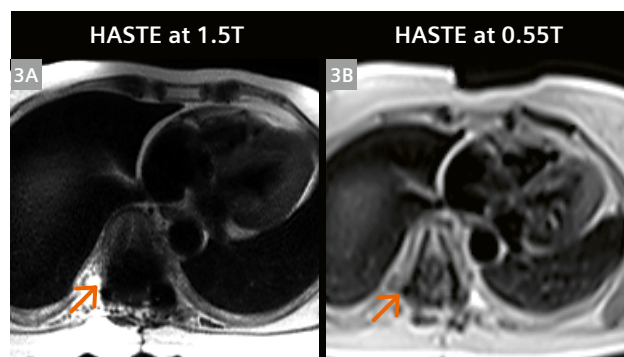
straightforward, and the technique performed well at low field with little modification. Example images in a healthy volunteer are shown in Figure 2, demonstrating the commonly used variants of black-blood T1 and T2-weighted TSE, and STIR. These are standard acquisitions with each 2D slice acquired in a short breath-hold of 10 to 12 heartbeats, and employed the Deep Resolve AI-based image denoising technique provided by Siemens Healthineers. Exemplary scan parameters used at 0.55T and 1.5T are listed in Table 1. Example images (Fig. 3) at both 1.5T and 0.55T in a patient with Harrington rods in their spine illustrate the reduced artifact surrounding metal implants² that can be expected at lower B₀ field strength.

Cine

Cine imaging is at the core of every CMR exam, providing information on cardiovascular morphology and function. Measurements can be made on the cine images to quantify global and regional cardiac function. Cine typically relies on balanced steady-state free precession, (bSSFP) and therefore has inherently high SNR relative to other techniques. Thus, the reduced SNR at low field is not a significant obstacle; however, bSSFP cine does require short TR for high temporal resolution, thus presenting a challenge on this scanner where gradient performance is limited. We have addressed this challenge through the utilization of CS reconstruction methods [9]. Table 2 lists the imaging parameters achieved at 0.55T, in comparison to a 1.5T scanner with faster gradients. With highly accelerated CS-based sequences, we have been able to achieve high-quality cine results with segmented breath-hold techniques, as well as real-time, free-breathing imaging. Segmented *k*-space, breath-hold cine images acquired in the same patient at 1.5T and at 0.55T are shown in Figure 4. This patient has an artificial aortic valve with metallic components². The size of the signal void around the valve is less in the 0.55T images, as might be expected due to the reduced susceptibility gradients surrounding the metal. The degree of metal artifact is highly dependent on the specific material used to construct the implant².



2 Dark-blood images acquired in a volunteer. Single-shot HASTE images in different cardiac views are shown in the top row (2A). The bottom row shows T1 TSE, T2 TSE and T2 TSE STIR images in a mid-short axis view (2B). Each TSE image was acquired in a 12-heartbeat breath-hold.



3 Single-shot axial images acquired in a patient with Harrington rods post spinal fusion². HASTE images acquired on a 1.5T MAGNETOM Avanto system (3A) from a prior exam demonstrate significant susceptibility artifact (orange arrows) compared to localized artifact on the corresponding HASTE image at 0.55T (3B).

	Scanner	Flip angle (deg)	TE (ms)	Echo spacing (ms)	RBW Hz/pixel	Turbo factor	Temporal resolution (ms)	Slice thickness (mm)	Pixel size (mm)	Acceleration	Scan time
T2 TSE	1.5T MAGNETOM Sola	180	60	3.54	849	17	60	5	1.3 × 1.3	G 2	10 HB
	0.55T MAGNETOM Free.Max	180	43	5.36	401	14	75	6	2.0 × 2.0	G 2	12 HB
HASTE	1.5T MAGNETOM Sola	120	35	3.94	501	104	409	6	1.3 × 1.3	none	1 HB
	0.55T MAGNETOM Free.Max	160	16	4.1	1502	72	295	10	3.6 × 3.6	G 2	1 HB

Table 1: Acquisition parameters for breath-hold segmented turbo spin echo (TSE) (top rows) and single-shot HASTE (bottom rows) shown for 1.5T MAGNETOM Sola and 0.55T MAGNETOM Free.Max.

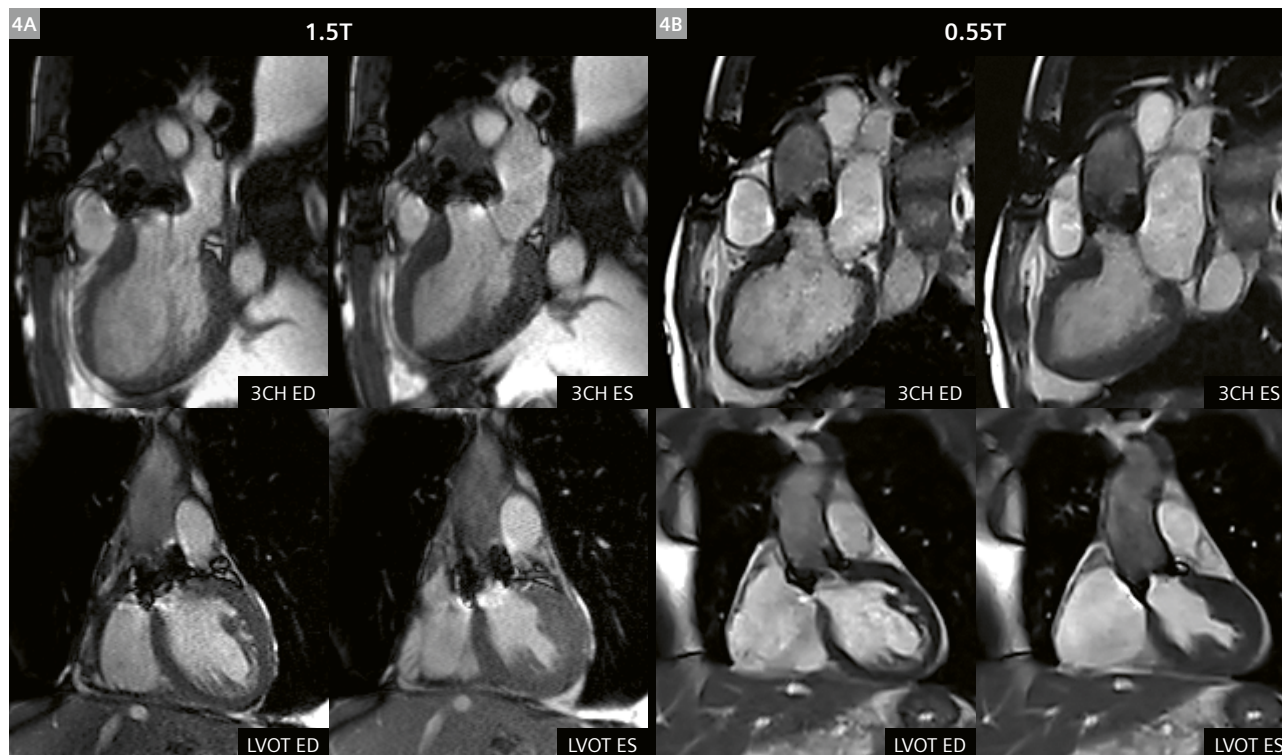
It is also dependent on TE and TR, and therefore will be affected by gradient performance as well as field strength. Figure 5 shows a comparison of breath-held segmented *k*-space cine images and real-time cine images, all acquired at 0.55T using the scan parameters listed in Table 2. Despite the high acceleration rates used to overcome slower gradient performance, SNR and overall image quality are maintained with CS reconstruction.

Flow quantification

Phase contrast (PC) imaging is the standard MRI method used to measure blood flow. While low-field offers advantages of reduced susceptibility and greater field homogeneity, the inherently low SNR of the spoiled gradient echo (GRE) sequences used for PC MRI can be challenging at low-field, and higher acceleration is needed to overcome slower gradients. We have successfully implemented segmented *k*-space, breath-hold flow quantification on the MAGNETOM Free.Max [10] and sample results

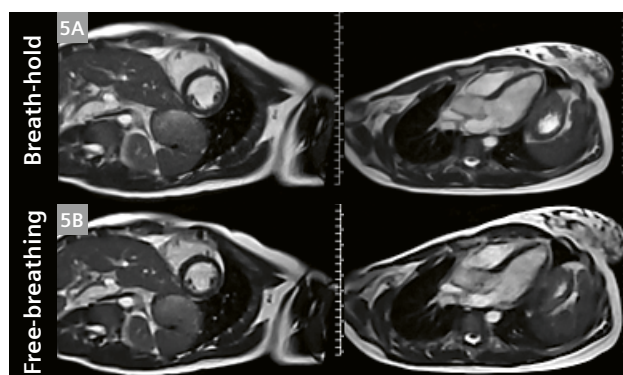
	Scanner	Flip angle (deg)	TE (ms)	TR (ms)	RBW Hz/pixel	Segments	Temporal resolution (ms)	Slice thickness (mm)	Pixel size (mm)	Acceleration	Scan time
BH-Cine	1.5T MAGNETOM Sola	75	1.16	2.71	930	12	32.5	6	1.8 × 1.8	CS 4.3	3 HB
	0.55T MAGNETOM Free.Max	110	1.95	4.65	930	6	27.9	8	1.8 × 1.8	CS 4.3	6 HB
RT-Cine	1.5T MAGNETOM Sola	75	1.04	2.43	1184	18	43.7	8	2.0 × 2.0	CS 7.4	1 HB
	0.55T MAGNETOM Free.Max	110	1.84	4.55	1002	10	45.5	8	2.0 × 2.0	CS 9.7	1 HB

Table 2: Acquisition parameters for breath-held segmented *k*-space cine (top rows) and real-time free-breathing cine (bottom rows) shown for 1.5T MAGNETOM Sola with faster gradients than the 0.55T MAGNETOM Free.Max. Higher acceleration rates are used for real-time cine on the MAGNETOM Free.Max to overcome the slower gradients.



4 End-diastole (ED) and End-systole (ES) cine frames acquired in a three-chamber view (3CH) and left ventricular outflow tract (LVOT) are shown. The 1.5T (MAGNETOM Avanto) (**4A**) images shown were acquired in the same patient in a prior exam using a GRAPPA-based breath-held segmented SSFP method. Images at 0.55T (**4B**) were acquired using a compressed sensing-based breath-held segmented SSFP method. Note that the patient has an artificial valve², and the metal artifacts in proximity to the valve are reduced at 0.55T.

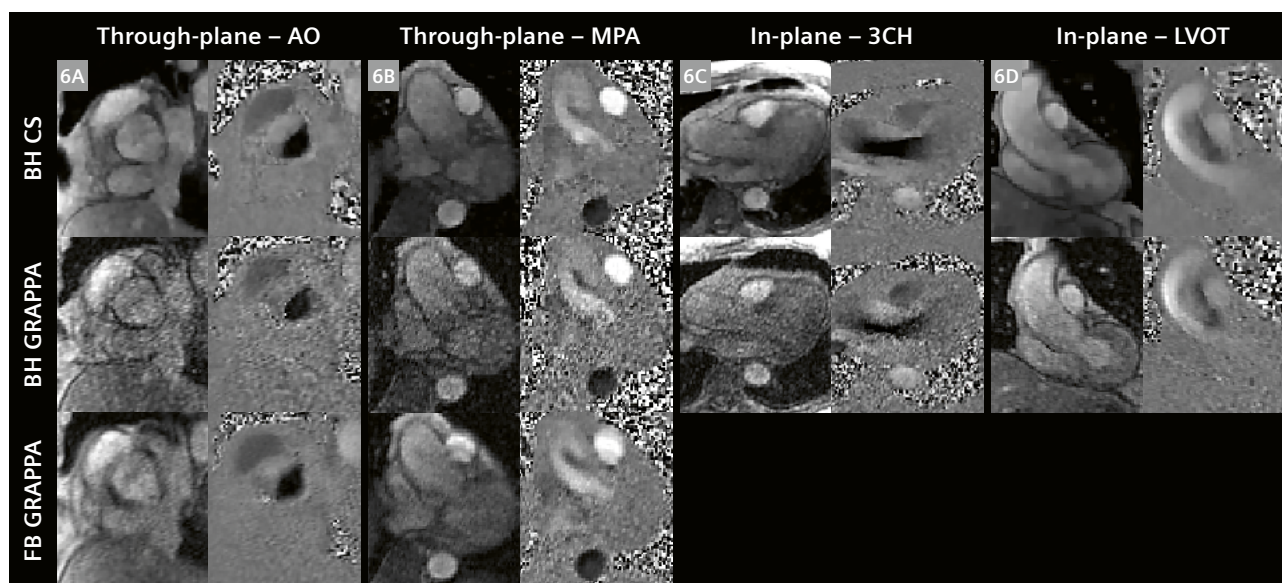
in comparison with GRAPPA parallel imaging are shown in Figure 6. In preliminary testing, CS-based reconstruction provides the high acceleration rates needed while maintaining spatial and temporal resolution and SNR. Real-time flow imaging requires significantly higher acceleration rates and is still under development, but free-breathing acquisition can be achieved through the use of signal averaging to suppress respiratory motion artifact, as also shown in Figure 6. Exemplary PC-MRI scan parameters are listed in Table 3. Although initial results demonstrate the feasibility of flow quantification on the MAGNETOM Free.Max, several sources of errors related to low-field and/or lower gradient performance (e.g., Maxwell-Terms and Flow Displacement Artifacts) are still under investigation.



5 Breath-held segmented *k*-space cine frames (**5A**) and real-time free-breathing cine frames (**5B**) acquired in a healthy volunteer. Despite use of a high under-sampling rate of near 10× in real-time cine, CS reconstruction provides sufficient image quality at 0.55T.

	Scanner	Flip angle (deg)	TE (ms)	TR (ms)	RBW Hz/pixel	Seg-ments	Temporal resolution (ms)	Slice thickness (mm)	Pixel size (mm)	Acceler-ation	Scan time
BH Flow	1.5T MAGNETOM Sola	15	2.26	4.23	501	5	42.3	6	2.0 × 2.0	G 2	10 HB
	0.55T MAGNETOM Free.Max	12	4.49	7.64	427	3	45.8	6	1.8 × 1.8	CS 3	13 HB
FB Flow	1.5T MAGNETOM Sola (RT)	12	2.51	4.41	560	6	52.9	10	2.8 × 2.8	CS 16	1 HB
	0.55T MAGNETOM Free.Max (avg)	12	3.67	6.55	427	3	39.3	8	1.9 × 1.9	G 2	58 HB

Table 3: Acquisition parameters for breath-hold segmented *k*-space flow quantification sequence (top rows) and free-breathing acquisition (bottom rows) shown for 1.5T MAGNETOM Sola and 0.55T MAGNETOM Free.Max. Free-breathing (FB) acquisition is currently achieved by signal averaging to suppress respiratory motion on MAGNETOM Free.Max, while real-time (RT) flow data acquisition is possible at 1.5T using compressed sensing. Real-time flow requires significantly higher acceleration, which is challenging in face of the reduced SNR at 0.55T.



6 Through-plane (**6A** aortic root and **6B** main pulmonary artery) and In-plane (**6C** 3-chamber view and **6D** left ventricular outflow tract) 2D phase contrast flow images acquired in a patient with a bicuspid aortic valve, aortic dilatation and aortic regurgitation. The top row shows magnitude and phase images acquired with a breath-held compressed sensing-based 2D PC MR sequence, while the middle row shows images from a breath-held GRAPPA sequence. Images in the bottom row were acquired free-breathing using a GRAPPA sequence with four averages to boost SNR. AO = aorta, MPA = main pulmonary artery, 3CH = cardiac 3-chamber view, LVOT = left ventricular outflow tract view.

Late Gadolinium Enhancement (LGE)

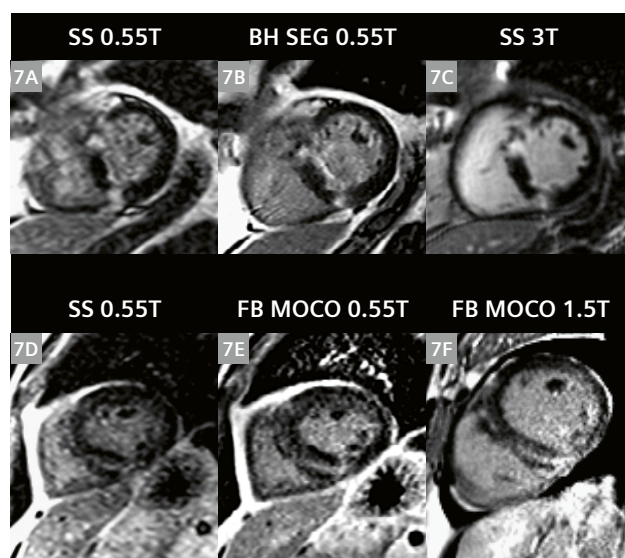
LGE provides unique information on myocardial tissue changes, including scar, fibrosis, and edema. We are currently optimizing both breath-hold segmented LGE and single-shot free-breathing LGE with motion correction and averaging, all based on bSSFP readout which provides high SNR. Exemplary scan parameters are listed in Table 4, along with 1.5T parameters for reference. Example images from two patients with non-ischemic cardiomyopathies showing segmented breath-hold, single-shot, and free-breathing, motion corrected LGE at 0.55T, along with comparative images acquired at 1.5T and 3T, are shown in Figure 7. Additional improvements in acquisition speed and image quality are anticipated as we incorporate compressed sensing into LGE image acquisition and reconstruction.

Gadolinium contrast agent T1 relaxivity is generally a function of field strength, and as shown by Campbell-Washburn et al., relaxivity at 0.55T may be slightly higher or lower than at 1.5T, depending on the particular agent [2]. All of the contrast-enhanced images shown here used gadobutrol, which may have a slightly lower (worse) relaxivity at 0.55T than at 1.5T. Additionally, because the native T1 times are shorter, the differential contrast enhancement at lower field may be less. Thus far, in our preliminary studies, we have observed the use of gadolinium-based contrast agent to be effective for the visualization of myocardial scar, perfusion defects, and blood pool in MRA, but careful studies are required to evaluate the diagnostic efficacy.

Myocardial relaxation parameter mapping

Myocardial longitudinal (T1) and transverse (T2) relaxation times are elevated with fibrosis, edema, and inflammation. Quantitative myocardial parameter mapping methods are being used clinically at higher field to evaluate these

pathological changes in myocardium that can accompany a variety of diseases. We implemented parameter mapping schemes for T1 and T2 taking into consideration the shorter T1 relaxation times and longer T2 relaxation times at 0.55T in comparison to higher field. The T1-mapping scheme was based on that typically used for post-contrast T1 mapping at 1.5T (4(1)3(1)2), with the addition of a fourth inversion pulse and two more images at the shorter



7 Top row (7A–7C) shows LGE images acquired in a patient with hypertrophic cardiomyopathy with fibrosis of the left ventricle. (7A) Single-shot inversion recovery prepared bSSFP image at 0.55T, (7B) breath-held segmented LGE image at 0.55T, and (7C) single-shot IR-prepared bSSFP LGE image acquired on a 3T MAGNETOM Vida system for comparison. Bottom row (7D–7F) shows LGE images acquired in a different patient with non-ischemic septal mid-wall fibrosis. Single-shot (7D) and free-breathing motion-corrected averaged (7E) LGE images were acquired on MAGNETOM Free.Max, while the corresponding MOCO LGE image, shown in (7F), was acquired on a 1.5T MAGNETOM Sola system.

	Scanner	Flip angle (deg)	TE (ms)	TR (ms)	RBW Hz/pixel	Seg-ments	Temporal resolution (ms)	Slice thickness (mm)	Pixel size (mm)	Acceleration	Scan time
BH LGE	1.5T MAGNETOM Sola (GRE)	20	1.55	4.06	465	31	142	8	1.4 × 1.4	none	8 HB
	0.55T MAGNETOM Free.Max (bSSFP)	80	2.48	6.66	200	21	140	10	1.6 × 1.6	none	12 HB
MOCO LGE	1.5T MAGNETOM Sola (bSSFP)	50	1.18	2.79	1085	86	240	8	1.4 × 1.4	G 2	16 HB
	0.55T MAGNETOM Free.Max (bSSFP)	50	1.84	4.69	698	63	295	8	1.5 × 1.5	G 2	24 HB

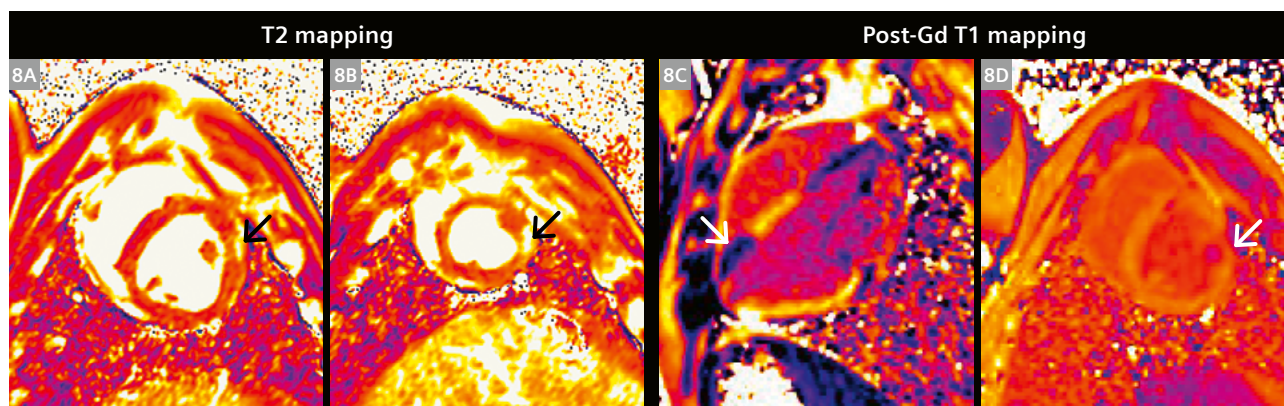
Table 4: Acquisition parameters for breath-hold segmented *k*-space LGE (top rows) and free-breathing LGE based on single-shot acquisition with motion correction (MOCO) and averaging (bottom rows) shown for 1.5T MAGNETOM Sola and 0.55T MAGNETOM Free.Max. Additional averages were used at 0.55T in the MOCO LGE scan to boost SNR. Note also that the standard segmented breath-hold approach at 1.5T and 3T typically utilizes a GRE readout, while bSSFP is employed at 0.55T to boost SNR. The higher B_0 homogeneity allows broader utilization of bSSFP without risk of dark band artifacts that could confound the interpretation of LGE, first pass perfusion, and other techniques where changes in myocardial signal intensity are of interest.

inversion times (4(1)3(1)2(1)2). The T2 mapping scheme was modified to acquire 6 source images at 3 different T2 preparation times (0, 25, and 60 ms). Scan parameters are listed in Table 5, along with typical parameters used at 1.5T for comparison. Results shown in Figure 8 acquired in a porcine infarct model at 0.55T utilized an increased number of source images to boost SNR through the pixel-wise parameter fitting process. We are continuing to work

on applying the same CS strategies that have been instrumental in boosting SNR and acceleration rates in cine and flow, and expect that this will improve SNR and sharpness in the resulting parameter maps, while reducing the scan duration. Prospective respiratory motion compensation techniques based on the Pilot Tone technology [11] are under development and will be used to further improve free-breathing methods.

	Scanner	Flip angle (deg)	TE (ms)	TR (ms)	RBW Hz/pixel	Segments	Temporal resolution (ms)	Slice thickness (mm)	Pixel size (mm)	Acceleration	Scan time
T1 mapping	1.5T MAGNETOM Sola	35	1.01	2.42	1085	60	145	8	2.0 × 2.0	G 2	11 HB
	0.55T MAGNETOM Free.Max	50	1.77	4.3	539	60	258	10	2.4 × 2.4	G 2	14 HB
T2 mapping	1.5T MAGNETOM Sola	70	1.04	2.43	1184	55	133	8	2.1 × 2.1	G 2	7 HB
	0.55T MAGNETOM Free.Max	70	1.69	4.18	558	60	250	10	2.4 × 2.4	G 2	16 HB

Table 5: Acquisition parameters for myocardial T1 mapping (top rows) and T2 mapping (bottom rows) listed for both 1.5T MAGNETOM Sola and 0.55T MAGNETOM Free.Max. Additional source images are acquired at 0.55T to boost SNR, leading to slightly longer scan times. Longer TR due to slower gradients also degrades temporal resolution, and this can cause some motion artifact at higher heart rates. Approaches to increase acceleration rate to improve temporal resolution are being developed using Compressed Sensing.



8 Myocardial T2 (8A, 8B) and post-Gd T1 (8C, 8D) maps acquired in a porcine model of acute myocardial infarction. These images, acquired five days post 90-minute occlusion-reperfusion of the left circumflex coronary artery, illustrate the feasibility of parameter mapping at 0.55T. Antero-lateral infarct is visible as regionally elevated T2 (black arrows in panels 8A and 8B), and shortened post-contrast T1 (white arrows in panels 8C and 8D).

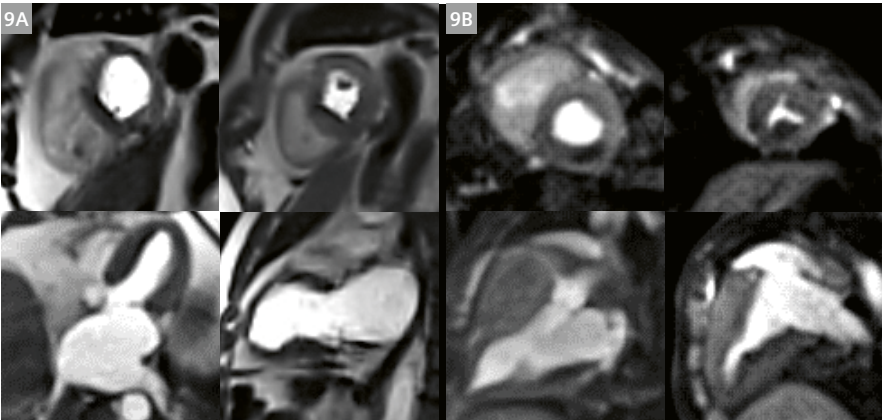
	Scanner	Flip angle (deg)	TE (ms)	TR (ms)	RBW Hz/pixel	Segments	Temporal resolution (ms)	Slice thickness (mm)	Pixel size (mm)	Acceleration	Scan time
First-pass Perfusion SR-bSSFP	1.5T MAGNETOM Sola (bSSFP)	50	1.04	2.5	1085	37	92.5	8	1.9 × 1.9	G 3	50 HB
	0.55T MAGNETOM Free.Max (bSSFP)	90	1.81	4.04	868	25	101	8	3.0 × 3.0	CS 4	50 HB

Table 6: Acquisition parameters for myocardial first-pass perfusion imaging for 1.5T MAGNETOM Sola (top row) and 0.55T MAGNETOM Free.Max (bottom row). Saturation-recovery (SR) bSSFP is used on both scanners. Compressed Sensing is used on MAGNETOM Free.Max to push the acceleration rate to 4× to overcome the longer TR, and to maintain SNR. Even with higher acceleration there is some compromise in spatial and temporal resolution when compared to 1.5T. Further investigation is required to determine the impact of these parameter differences.

First-pass perfusion

Gadolinium-enhanced first-pass perfusion imaging, combined with vasodilator stress, is the most critical component of the CMR evaluation of patients with known or suspected ischemic heart disease. With the requirements

of delivering multi-slice coverage within a single heartbeat, and high T1-contrast images with little motion artifact, first-pass perfusion imaging pushes the speed and SNR limits of CMR even at higher field. Whether or not these requirements can be met at lower field with reduced



9 Rest perfusion images indicate perfusion defect in a patient with hypertrophic cardiomyopathy (9A) and in a porcine model with left circumflex artery infarct (9B).

	Scanner	Flip angle (deg)	TE (ms)	TR (ms)	RBW Hz/pixel	Segments or turbo factor	Temporal resolution (ms)	Slice thickness (mm)	Pixel size (mm)	Acceleration	Scan time
non-contrast MRA navigator bSSFP	1.5T MAGNETOM Sola	90	1.45	3.38	592	35	118	1.3	1.6 × 1.6	G 2	78 HB
	0.55T MAGNETOM Free.Max	110	1.89	4.61	501	35	161	1.5	1.6 × 1.6	G 2	142 HB
non-contrast MRA navigator SPACE	1.5T MAGNETOM Sola	variable	23	1RR	744	35	130	1.3	1.3 × 1.3	G 2	205 HB
	0.55T MAGNETOM Free.Max	variable	23	1RR	630	25	214	1.3	1.6 × 1.6	G 2	289 HB
Gd ce-MRA ECG gated GRE	1.5T MAGNETOM Sola	30	1.25	2.97	591	100	297	1.4	1.4 × 1.4	CS 9	10 HB
	0.55T MAGNETOM Free.Max	30	1.71	3.68	781	80	294	1.5	1.6 × 1.6	CS 7	13 HB

Table 7: Acquisition parameters for 3D MR angiography (MRA) sequences used on the 1.5T MAGNETOM Sola and 0.55T MAGNETOM Free.Max. Three different techniques are listed: 3D navigator respiratory gated bSSFP (top rows), 3D navigator gated dark-blood SPACE (middle rows), and 3D contrast enhanced ECG-gated MRA. Some compromises are made in spatial resolution on the MAGNETOM Free.Max to offset reduced SNR and gradient speed.



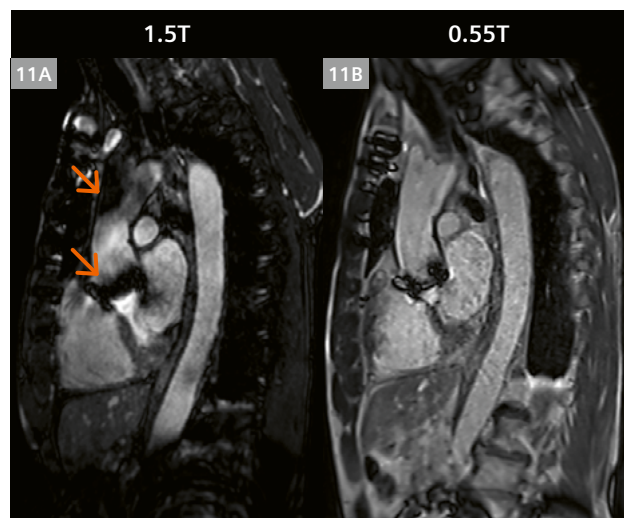
10 2D reformatted images from non-contrast 3D MRAs acquired in a patient with Harrington spinal rods² being evaluated for aortic dilatation. Images in (10A) show reconstructions from a bright-blood ECG-triggered, navigator gated bSSFP MRA, while (10B) shows reconstructions from a dark-blood 3D SPACE sequence used to highlight vessel wall anatomy.

gradient performance is an important question. We have experimented with a bSSFP perfusion sequence (parameters listed in Table 6) that applies the same CS-based approach to data sampling and reconstruction [9] that has been successfully utilized to accelerate real-time cine imaging without sacrificing SNR. While this method has yet to be tested with vasodilator stress, initial results acquired at rest in a porcine model of myocardial infarction, and in volunteers and patients, are promising (Fig. 9).

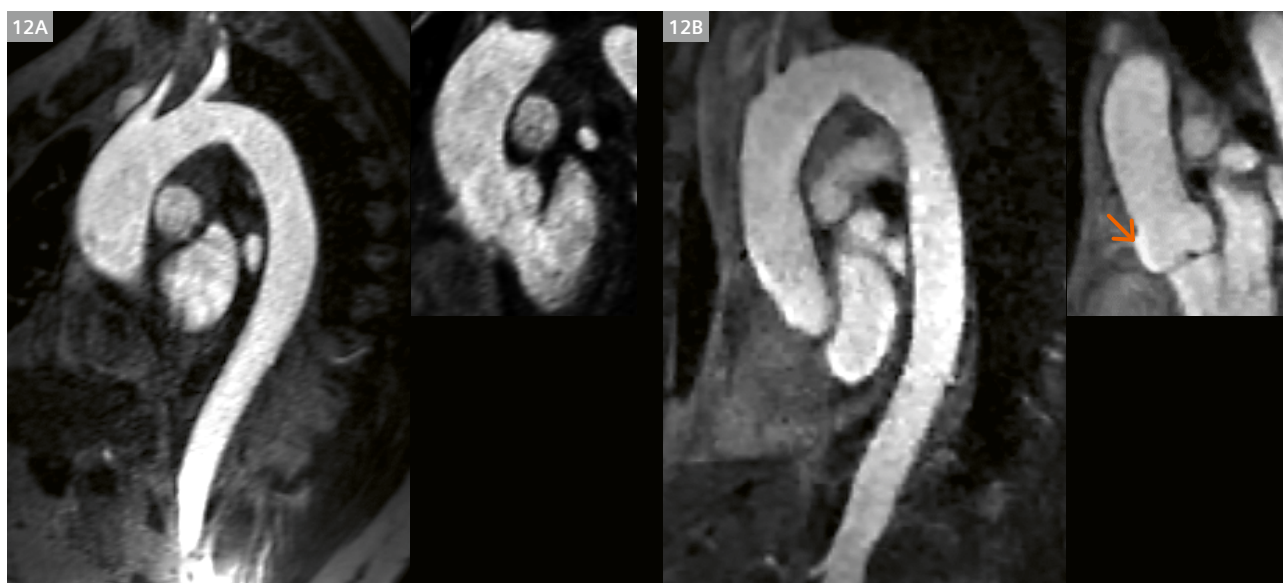
MR Angiography

Thoracic MR angiograms of the aorta, pulmonary arteries, and pulmonary veins form an important component of the comprehensive cardiovascular imaging exam in many of our patients. While the standard method is contrast-enhanced MR angiography (ce-MRA), non-contrast MRA using a 3D bSSFP sequence with navigator respiratory gating is now being utilized more frequently at our institution. We also frequently employ a 3D dark blood SPACE sequence to visualize vessel wall morphology; SPACE is also less sensitive to metal artifact around implants². Parameters for all three methods are listed in Table 7 for 0.55T and 1.5T. We have implemented and investigated all three of these MRA techniques in volunteers and patients. Contrast-enhanced MRA has been tested both with and without ECG gating, while the non-contrast technique is always ECG-triggered. ECG-gated ce-MRA places high demands on acceleration and we have employed a CS-based technique to maintain high spatial resolution and a reasonable breath-hold duration of 18 heartbeats or less.

Navigator-gated non-contrast MRA data were acquired during free-breathing with scan times of 6 minutes or less, depending on heart rate and the extent of anatomical coverage. 3D SPACE acquisition times are longer as signal averaging is used at both 1.5T and 0.55T. Examples of non-contrast and contrast-enhanced MRA acquired at 0.55T are shown in Figures 10, 11, and 12.



11 2D reformatted images from ECG triggered, navigator gated non-contrast enhanced 3D bSSFP MRA scans acquired in the same patient at 1.5T (**11A**) and at 0.55T (**11B**). This patient has an artificial aortic valve² and sternal wires. The extent of signal dephasing artifacts (orange arrows) seen at 1.5T are reduced at 0.55T. Cine images from this patient are shown in Figure 4.

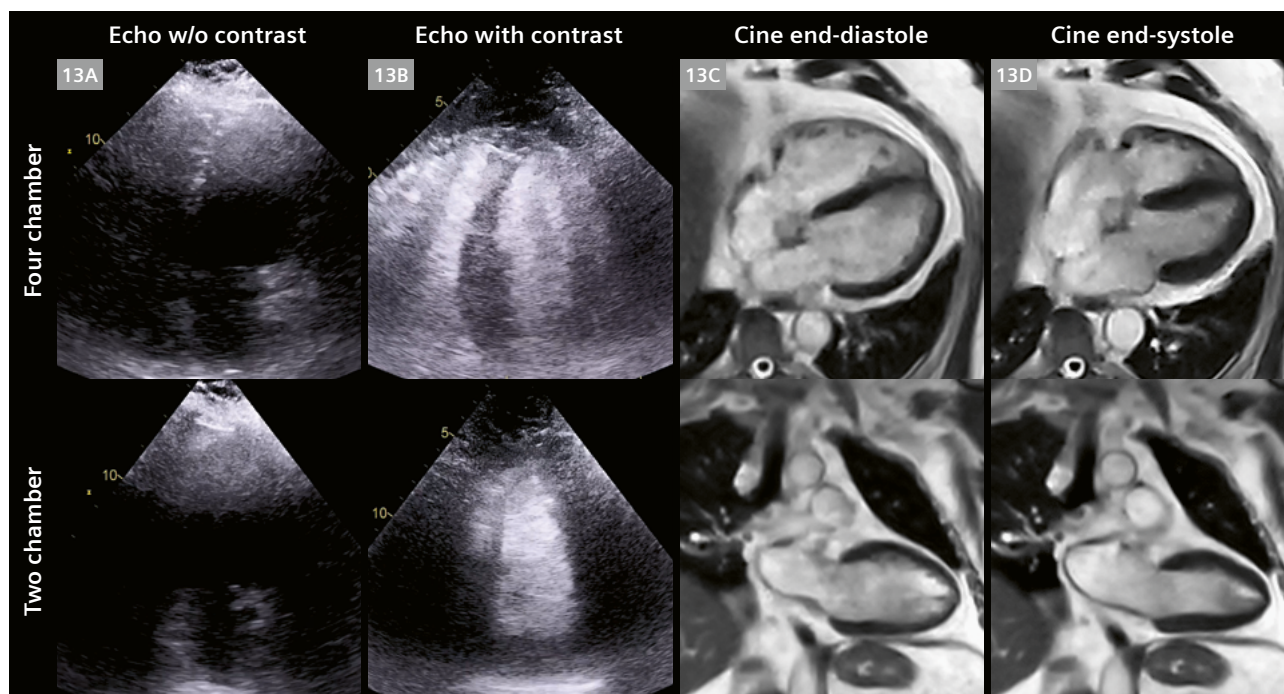


12 2D reformatted images from 3D contrast-enhanced (ce-)MRA scans in two different subjects. On the left (**12A**) a non-gated contrast-enhanced 3D MRA acquired in an obese patient shows a dilated thoracic aorta. The patient was unable to proceed with a cardiac MR exam in a standard 70 cm bore MR system but successfully completed an evaluation on the MAGNETOM Free.Max; additional images from this patient are shown in Figure 13. On the right (**12B**) is an ECG-gated ce-MRA scan from a healthy volunteer. Note the clear delineation of the aortic root and valve leaflets in the gated MRA (orange arrow), as compared to the non-gated MRA.

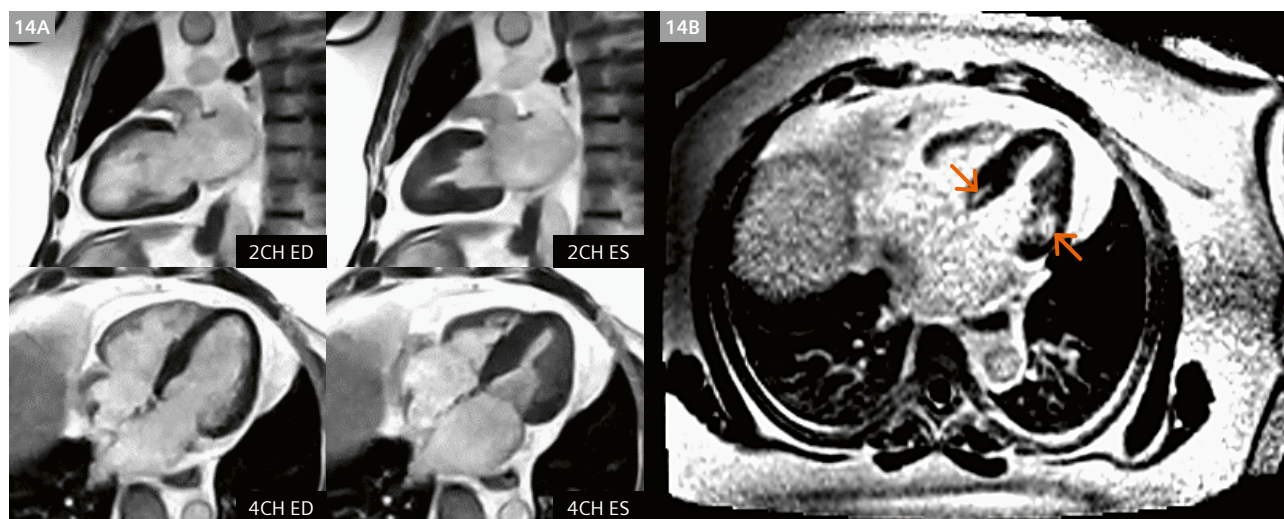
Putting it all together

After compiling the sequences required to cover all of the basic cardiac imaging applications, we have recently begun to identify and scan severely obese patients who were referred for clinical CMR, but whose body habitus made it

impossible, or too uncomfortable, to be scanned on systems with a standard 70 cm bore diameter. In Figure 13, images acquired on the MAGNETOM Free.Max are shown from a patient weighing 350 lbs / 159 kg with BMI > 48 being evaluated for possible cardiomyopathy and dilated



13 4-chamber view (top row) and 2-chamber view (bottom row) echocardiographic (13A without contrast, and 13B with contrast) and CMR images (13C end-diastole, and 13D end-systole) acquired in an obese patient with BMI > 48 kg/m². Echo image quality is degraded by large body habitus, and this patient could not fit into a 70 cm magnet bore. The MAGNETOM Free.Max provides access to MRI for severely obese patients for whom no other good options exist for cardiac imaging. MRA for this patient is shown in Figure 12.



14 Example images from a patient weighing 410 lbs / 186 kg with BMI 57 kg/m². This patient being evaluated for cardiomyopathy, was unable to complete the exam on a 70 cm bore system. Compressed Sensing-based breath-held segmented bSSFP cine images acquired on the MAGNETOM Free.Max are shown in panel (14A) on the left. End-diastolic and end-systolic cardiac phases are shown. In panel (14B) on the right is shown an LGE image acquired during free-breathing using the technique of single-shot motion corrected (MOCO) imaging with averaging. Basal regions of enhancement (orange arrows) indicate areas of fibrosis.

aorta. While the weight of this patient can be accommodated by most scanners, their body habitus prevented them from fitting into a 70 cm bore. They were comfortably scanned on the MAGNETOM Free.Max, and the bSSFP cine images are shown here in comparison to echocardiography images acquired with and without echo contrast. The echo image quality is poor, and MAGNETOM Free.Max offers the potential for high-quality cardiac imaging for these severely obese patients in whom other modalities including echo and CT may be limited. The contrast-enhanced MR angiogram acquired in this patient is shown in Figure 12. MAGNETOM Free.Max images from another patient with a BMI of 57 (weight 410 lbs / 186 kg) diagnosed with heart failure with preserved ejection fraction (HFpEF) being evaluated for cardiomyopathy are shown in Figure 14. This patient was able to initially enter the bore of a 70 cm scanner, but was too uncomfortable to complete the exam. The patient reported being comfortable in the MAGNETOM Free.Max. The exam, including cine and LGE imaging was successfully completed, revealing normal biventricular function, but scarring evident at the base of the left ventricle.

Summary

While this project to develop and optimize cardiac imaging techniques for the 0.55T MAGNETOM Free.Max is still in relatively early stages, the images and results obtained thus far show great promise for the breadth of techniques and image quality that this system will be able to deliver in the future. We will continue to explore the cardiac imaging potential for this ultra-wide bore 0.55T system and anticipate that in the near future it will provide a solution to accurately diagnose and guide clinical cardiovascular care of patients with severe obesity, as well as those with severe claustrophobia.

Acknowledgements

The entire OSU CMR team, and Siemens Healthineers collaborators. Funding support from National Heart Lung and Blood Institute (R01HL161618) and The Robert F. Wolfe and Edgar T. Wolfe Foundation. Columbus, Ohio, USA.

References

- 1 Simonetti OP, Ahmad R. Low-Field Cardiac Magnetic Resonance Imaging: A Compelling Case for Cardiac Magnetic Resonance's Future. *Circ Cardiovasc Imaging*. 2017;10(6):e005446.
- 2 Campbell-Washburn AE, Ramasawmy R, Restivo MC, Bhattacharya I, Basar B, Herzka DA, et al. Opportunities in Interventional and Diagnostic Imaging by Using High-Performance Low-Field-Strength MRI. *Radiology*. 2019;293(2):384-393.
- 3 Hales CM, Carroll MD, Fryar CD, Ogden CL. Prevalence of Obesity and Severe Obesity Among Adults: United States, 2017-2018. *NCHS Data Brief*. 2020;(360):1-8.
- 4 Virani SS, Alonso A, Aparicio HJ, Benjamin EJ, Bittencourt MS, Callaway CW, et al. Heart Disease and Stroke Statistics-2021 Update: A Report From the American Heart Association. *Circulation*. 2021;143(8):e254-e743.
- 5 Fursevich DM, Limarzi GM, O'Dell MC, Hernandez MA, Sensakovic WF. Bariatric CT Imaging: Challenges and Solutions. *RadioGraphics*. 2016;36(4):1076-1086.
- 6 Finkelhor RS, Moallem M, Bahler RC. Characteristics and impact of obesity on the outpatient echocardiography laboratory. *Am J Cardiol*. 2006;97(7):1082-1084.
- 7 Varghese J, Craft J, Crabtree CD, Liu Y, Jin N, Chow K, Ahmad R, Simonetti OP. Assessment of cardiac function, blood flow and myocardial tissue relaxation parameters at 0.35 T. *NMR Biomed*. 2020;33(7):e4317.
- 8 Bandettini WP, Shanbhag SM, Mancini C, McGuirt DR, Kellman P, Xue H, et al. A comparison of cine CMR imaging at 0.55 T and 1.5 T. *J Cardiovasc Magn Reson*. 2020;22(1):37.
- 9 Chen C, Liu Y, Schniter P, Jin N, Craft J, Simonetti O, et al. Sparsity adaptive reconstruction for highly accelerated cardiac MRI. *Magn Reson Med*. 2019;81(6):3875-3887.
- 10 Jin N, Liu Y, Chen C, Giese D, Ahmad R, Simonetti O. Highly accelerated 2D phase contrast imaging on a low-field 0.55T MRI system. *ISMRM Workshop on Low Field MRI*, March 2022.
- 11 Speier P, Fenchel M, Rehner R. PT-Nav: a novel respiratory navigation method for continuous acquisitions based on modulation of a pilot tone in the MR-receiver. *ESMRMB 2015, 32nd Annual Scientific Meeting*, Edinburgh, UK, 1-3 October: Abstracts, Thursday, Magnetic Resonance Materials in Physics, Biology and Medicine. 2015; 28:1-135.



Contact

Orlando P. Simonetti, PhD, MScMR, FISMRM, FAHA
John W. Wolfe Professor of Cardiovascular Research
Professor of Internal Medicine and Radiology
The Ohio State University
Biomedical Research Tower
460 W. 12th Ave.
Columbus, OH 43210
USA
Tel.: +1 614-293-0739
Orlando.Simonetti@osumc.edu